JOURNAL OF VIROLOGY, Dec. 1997, p. 9270–9277 Vol. 71, No. 12
0022-538X/97/$04.00+0

DNA-Dependent Transregulation by IE1 of *Autographa californica* Nuclear Polyhedrosis Virus: IE1 Domains Required for Transactivation and DNA Binding

STEVEN M. RODEMS,† STEVEN S. PULLEN,‡ AND PAUL D. FRIESEN*

Institute for Molecular Virology and Department of Biochemistry, Graduate School and College of Agricultural and Life Sciences, University of Wisconsin—Madison, Madison, Wisconsin 53706

Received 18 July 1997/Accepted 10 September 1997

IE1 is the principal early transregulator of *Autographa californica* multicapsid nuclear polyhedrosis virus (Ac*M*NPV). The 582-residue protein stimulates viral transcription and binds as a dimer to 28-bp palindromic repeats (28-mers) comprising the Ac*M*NPV homologous region (*hr*) transcription enhancers. To define IE1 domains responsible for *hr*-dependent transactivation, we first constructed a series of IE1 fusions to the DNA binding domain of the yeast GAL4 transactivator. In transfection assays, GAL4-IE1 fusions stimulated transcription from a TATA-containing Ac*M*NPV promoter only upon *cis* linkage to GAL4 DNA binding sites. IE1 N-terminal residues 8 to 118 were sufficient for GAL4-binding-site-dependent transactivation. To identify IE1 residues required for *hr* interaction, we tested a series of IE1 mutations for 28-mer binding by using electrophoretic mobility shift assays. Deletion of IE1 residues other than the N-terminal transactivation domain eliminated 28-mer binding. Of 14 insertion mutations, only IE1^{I425} and IE1^{I553} failed to bind the 28-mer either as homodimers or as heterodimers with functional IE1. In contrast to insertion IE1^{I425}, IE1^{I553} also failed to compete with wild-type IE1 for DNA binding and suggested a defect in oligomerization. Consistent with loss of oligomerization, substitutions within a hydrophobic repeat (residues 543 to 568) at the IE1 C terminus abolished 28-mer binding and demonstrated that this helix-loop-helix-like domain is required for DNA interaction. These data confirm that IE1 contains separable domains for transactivation and oligomerization-dependent DNA binding. Furthermore, they support a model wherein *hr*-mediated transactivation by IE1 involves sequence-specific DNA binding that contributes to transcriptional stimulation by interaction with components of the basal transcription complex.

Current evidence indicates that immediate-early gene 1 (*ie-1*) is the principal transregulator of early gene expression by the baculovirus *Autographa californica* multicapsid nuclear polyhedrosis virus (Ac*M*NPV). The 67-kDa *ie-1* gene product (IE1) is a potent transactivator of early viral genes in plasmid transfection assays (3, 16, 18, 24, 31, 35, 44). Moreover, *ie-1* is required in plasmid replication assays and thus may contribute directly or indirectly to viral DNA replication (21, 32). Lastly, as indicated by replication defects exhibited by the Ac*M*NPV mutant *ts*B821, carrying a temperature-sensitive lesion in *ie-1*, IE1 is required for proper timing of Ac*M*NPV replication (7, 43). Despite these apparent contributions of IE1 to productive baculovirus infection, the molecular mechanisms of IE1 function are poorly understood.

As assayed by plasmid transfections, IE1-mediated transcriptional activation is significantly amplified when the affected promoter is *cis* linked to homologous region (*hr*) enhancer sequences from Ac*M*NPV (3, 15, 17, 31, 35, 39, 44). Ranging in size from 30 to 800 bp, eight *hr* enhancer elements are dispersed throughout the circular Ac*M*NPV genome (134 kbp) (1, 8) and may function as origins of viral DNA replication (22, 28, 36). The 28-bp palindromic repeats (28-mer) comprising the *hr*s are the minimal sequence required for orientation- and position-independent enhancer activity (44, 45) and *hr*-mediated plasmid DNA replication (28, 36). IE1 interaction with the *hr*s is mediated in part by the palindromic 28-mers (6, 13, 14, 26, 45). In particular, nucleotide substitutions within the 28-mer that eliminate IE1 binding also abolish 28-mer-mediated transactivation (45) and transient DNA replication (26). Thus, IE1 stimulation of *hr*-mediated enhancement or DNA replication may require IE1 binding to *hr* sequences.

IE1 binds to the palindromic 28-mer as a dimer, and optimal IE1 interaction requires both 28-mer half-sites (45). Although a single half-site is sufficient for IE1 interaction, both half-sites with a precise spacing are required for enhancer activity and DNA replication (14, 26, 44, 45). Thus, a critical step in IE1 function is the proper interaction of oligomeric IE1 with the 28-mer. However, the molecular events by which IE1 subsequently stimulates *hr*-dependent transcription or DNA replication are unknown. Essential to defining these IE1-mediated events is the identification and characterization of the protein domains involved.

To first test the hypothesis that IE1 binding to DNA contributes to *hr* enhancer activity, we constructed a series of fusions between IE1 and the DNA binding domain (DBD) of the yeast GAL4 transcriptional activator. This strategy enabled us to investigate IE1 transactivation in response to DNA binding mediated independently by the GAL4 DBD and thereby map IE1 residues sufficient for transactivation. We report here that GAL4-IE1 fusions stimulated TATA-dependent transcription but only when the promoter was *cis*-linked to GAL4

* Corresponding author. Mailing address: Institute for Molecular Virology, Bock Laboratories, University of Wisconsin—Madison, 1525 Linden Dr., Madison, WI 53706-1596. Phone: (608) 262-7774. Fax: (608) 262-7414. E-mail: PFriesen@facstaff.wisc.edu.

† Present address: Department of Biology, University of California, San Diego, La Jolla, CA 92093-0357.

‡ Present address: Boehringer Ingelheim Pharmaceuticals, Inc., Ridgefield, CT 06877.

DNA binding sites. N-terminal IE1 residues 8 to 118 were sufficient for maximal GAL4-IE1 transactivation. These findings confirmed and extend a deletion analysis by Kovacs et al. (23), which showed that the N and C termini of IE1 are required for transactivation and *hr* complex formation, respectively. Thus, to further distinguish IE1 residues required for transactivation and oligomerization-dependent DNA binding, we tested the capacity of an extensive series of IE1 mutations to bind to an *hr*5 28-mer-containing DNA probe in electrophoretic mobility shift assays (EMSAs). To avoid potential problems of intracellular instability, we synthesized mutated forms of IE1 in vitro and thereby identified several regions required for 28-mer interaction. In particular, mutations within a 4-3 repeat of hydrophobic residues (34) near the IE1 C terminus eliminated DNA binding as well as the capacity to compete with wild-type IE1 for the 28-mer. Collectively, these data indicate a critical role for IE1 oligomerization in *hr* enhancer activity. Moreover, they are consistent with a model in which localization of the N-terminal IE1 transactivation domains to the basal transcription complex by DNA binding contributes to stimulation of early viral transcription.

MATERIALS AND METHODS

Cells and transfections. *Spodoptera frugiperda* IPLB-SF21 (SF21) (54) cells were propagated in TC100 growth medium (GIBCO Laboratories) supplemented with 2.6 mg of tryptose broth per ml and 10% heat-inactivated fetal bovine serum. Calcium phosphate transfections of plasmid DNA were performed as described previously (39, 45).

Plasmid construction. (i) GAL4-IE1 expression plasmids. pIE1prm/GAL4-DBD was constructed by inserting the 542-bp *Hin*dIII-*Bam*HI fragment (end repaired) that contains the GAL4 DBD (amino acid residues 1 to 147) and the influenza virus hemagglutinin epitope of plasmid pAS2 (57) into end-repaired *Bgl*II and *Bst*BI sites downstream of the *ie-1* promoter (nucleotides −546 to +32 relative to the RNA start site, +1) of plasmid $pIE1_{Bg2}$ (39). Insertion of the *ie-1*-containing 2,038-bp *Mlu*I-*Bam*HI fragment (end repaired) from pSP64/IE1 (45) into the *Sma*I site of pAS2 generated pAS2/IE1(8-582). Construction of pIE1prm/GAL4-IE1(8-582) was identical to that of pIE1prm/GAL4-DBD except that the inserted 2,584-bp *Hin*dIII-*Bam*HI fragment was derived from pAS2/IE1(8-582). pIE1prm/GAL4-DBD(ΔMCS) was derived by *Sal*I and *Xba*I digestion of pIE1prm/GAL4-DBD, end repair with Klenow fragment, and religation. pIE1prm/GAL4-DBDx was generated by *Bam*HI digestion, end repair with Klenow fragment, and ligation to an *Xba*I amber stop codon linker (5′-CTAGTCT AGACTAG-3′). pIE1prm/GAL4-IE1(8-51), pIE1prm/GAL4-IE1(8-217), and pIE1prm/GAL4-IE1(53-217) were constructed by insertion of end-repaired *Mlu*I-*Eco*RV, *Mlu*I-*Nde*I, and *Eco*RV-*Nde*I fragments, respectively, from pSP64/IE1 into the *Sma*I site of pIE1prm/GAL4-DBDx. pIE1prm/GAL4-IE1(120-217) was constructed by insertion of an end-repaired *Nde*I-*Bsm*I fragment from pSP64/IE1 into the *Nco*I site of pIE1prm/GAL4-DBDx. *Nde*I digestion of pIE1prm/GAL4-IE1(8-582) and intramolecular ligation generated pIE1prm/GAL4-IE1(217-582). The chloramphenicol acetyltransferase (CAT) reporter plasmid $pG_5 35K_{BAS}$-CAT/PA was generated by inserting the end-repaired *Hin*dIII-*Xba*I fragment, containing five GAL4 binding sites, from plasmid $(GAL4)_5$/E1bTATA (29) into the end-repaired *Bgl*II site of pBAS35K-CAT/PA (44).

(ii) *ie-1* deletions. pSP64/IE1 (45) was digested with *Dra*III and *Eco*RV or *Stu*I, end repaired with T4 DNA polymerase, and ligated to 8-bp *Pst*I linkers (5′-CCTGCAGG-3′) to generate $pSP64/IE^{\Delta 53\text{-}143}$ and $pSP64/IE1^{\Delta 144\text{-}155}$, respectively. pSP64/IE1 was digested with *Eco*47III and *Stu*I or *Eco*RV and *Nde*I, end repaired with Klenow fragment, and religated to create $pSP64/IE^{\Delta 13\text{-}156}$ and $pSP64/IE1^{\Delta 53\text{-}217}$, respectively. pIE1/BS (39) was digested with *Bsm*BI and *Nde*I or *Swa*I, end repaired with Klenow fragment, and religated. The *Eco*RV-*Xba*I fragments from resulting plasmids were inserted into the corresponding sites of pSP64/IE1 to generate $pSP64/IE^{\Delta 218\text{-}293}$ and $pSP64/IE1^{\Delta 295\text{-}414}$. $pSP64/IE^{\Delta 415\text{-}513}$ was constructed by *Swa*I digestion of pSP64/IE1, followed by partial digestion with *Acc*I, end repair with Klenow fragment, and intramolecular ligation. pSP64/IE1 was digested with *Dra*III, end repaired with T4 DNA polymerase, and religated to generate $pSP64/IE1^{143\Delta}$. $pSP64/IE1^{\Delta 9\text{-}52}$ (also designated pSP64/$IE1^{\Delta}$) was described previously (45).

(iii) *ie-1* insertions. All insertions were generated from pSP64/IE1. Digestion with *Stu*I or *Swa*I and ligation to 12-bp *Bgl*II linkers (5′-GGAAGATCTTCC-3′) generated $pSP64/IE1^{I156}$ and $pSP64/IE1^{I414}$, respectively. Digestion with *Acc*I or *Bst*BI, end repair with Klenow fragment, and ligation to 10-bp *Bgl*II linkers (5′-GAAGATCTTC-3′) generated $pSP64/IE1^{I513}$ and $pSP64/IE1^{I579}$, respectively. $pSP64/IE1^{I118}$ and $pSP64/IE1^{I143}$ were constructed by digestion with *Bsm*I or *Dra*III, end repair with T4 DNA polymerase, and ligation to 8-bp (5′-CAG ATCTG-3′) and 12-bp *Bgl*II linkers, respectively. Partial digestion with *Hpa*I, *Bsa*AI, and *Ssp*I and ligation to 12-bp *Bgl*II linkers generated $pSP64/IE1^{I70}$ and $pSP64/IE1^{I418}$, $pSP64/IE1^{I243}$ and $pSP64/IE1^{I425}$, and $pSP64/IE1^{I391}$ and $pSP64/IE1^{I553}$, respectively. $pSP64/IE1^{I70}$ contains two linkers in which the downstream linker has a single-base (underlined) substitution (5′-GGAAGATCTTC-3′). $pSP64/IE1^{I311}$ was constructed by partial digestion with *Alw*44I, end repair with Klenow, and ligation to 8-bp *Bgl*II linkers. $pSP64/IE1^{I462}$ was constructed by partial digestion with *Sph*I, end repair with T4 DNA polymerase, and ligation to 10-bp *Bgl*II linkers. Amino acid residues inserted (bold) at the site of each mutation are indicated: I70, L_{70}**EDLPEDL**ST_{71}; I118, F_{118}**ADL**H_{120}; 143Δ, S_{143}**RV**$_{146}$; I143, S_{143}**RKIFRV**$_{146}$; I156, R_{156}**GRSSP**$_{157}$; I243, Y_{243}**GRSSV**$_{244}$; I311, H_{311}**RSVH**H_{312}; I391, Q_{391}**MEDLPL**$_{393}$; I414, L_{414}**EDLP**N_{415}; I418, V_{418}**GRSSN**$_{419}$; I425, T_{425}**EDLPY**$_{426}$; I462, G_{462}**RKIF**H_{465}; I513, V_{513}**GRSSD**$_{514}$; I553, L_{553}**MEDLPL**$_{555}$; and I579, F_{579}**GRSSE**$_{580}$.

(iv) *ie-1* substitutions. pIE1/BS was modified by site-directed mutagenesis (25) using oligonucleotides 5′-CCGATTACAAACATATGATGCGCAAATGCAT TATATTTTTG-3′, 5′-GCAATGTAGTGCTCTCTGCTGCGTTAACTTTAC CGATTAC-3′, 5′-TAAAGCTAACAATTTGAGCTCATTATTGTGGTCTGT AGTGCTCTC-3′, 5′-CGGAACCAGACCCTGGAGCTCTAAAGCTAAGTC TTTTAACAAATTATTG-3′, 5′-CCGCAAACGTTATTTCGTCGGAGTCCG GTACCAGACCCTGTAATAT-3′, and 5′-TTTATATTTACAATTAAGCTTT TGTTCCTCAAACGTGTCAGCGTCGGACAA-3′ (nucleotide substitutions are underlined). The 344-bp *Sph*I-*Bst*BI fragment of the resulting plasmids was inserted into the corresponding sites of pSP64/IE1 to generate pSP64/IE1(524/526), pSP64/IE1(537/538), pSP64/IE1(543/547), pSP64/IE1(550/554), pSP64/IE1(561/564), and pSP64/IE1(565/568), respectively. All mutations were verified by nucleotide sequencing.

CAT assays. Freeze-thaw extracts from plasmid-transfected SF21 cells were assayed for CAT as described previously (10). Acetylation of [^{14}C]chloramphenicol was quantified by using a PhosphorImager (Molecular Dynamics).

In vitro protein synthesis. Rabbit reticulocyte lysates were used in coupled in vitro transcription-translation reactions according to the manufacturer's protocol (TNT system; Promega). Circular plasmid templates (200 ng) were added singly or together to a reaction mixture (10 μl) containing reticulocyte lysate, amino acids, SP6 polymerase, and RNasin (Promega). After a 1.5-h incubation at 30°C, reactions were adjusted to a final concentration of 15% glycerol and stored at −80°C. To radiolabel in vitro-synthesized proteins, reactions were supplemented with Tran^{35}S-label (ICN).

28-mer-containing *hr*5 DNA probe. The primers 5′-CACACAGGAAACAG CTATGAC-3′ and 5′-CGGCCAGTGAATTGTAATACG-3′ were used to PCR amplify sequences of plasmid p*hr*5DA(−) (45). The 28-mer-containing PCR fragment was purified by using Wizard PCR Preps (Promega) and digested with *Xba*I and *Xho*I. The resulting 131-bp fragment was dephosphorylated, purified by agarose gel electrophoresis, and end labeled with T4 kinase and [α-^{32}P]ATP.

EMSAs. Protein-DNA complexes using in vitro-synthesized IE1 and the 28-mer DNA probe were subjected to nondenaturing 5% polyacrylamide–Tris-glycine gel electrophoresis for 3 to 5 h as described previously (45).

Image processing. Autoradiograms were scanned at a resolution of 300 dots/in. by using a Microtek Scanmaker III equipped with a transparency adapter. The resulting files were printed from Adobe Photoshop 3.0 by using a Tektronix Phaser 440 dye sublimation printer.

RESULTS

IE1 transactivation through direct DNA binding. Mutations within the *hr*5 28-mer that disrupt IE1 binding and eliminate 28-mer-mediated transcriptional activation support a model wherein IE1 transactivation involves sequence-specific DNA binding (23, 45). To test IE1's capacity to transactivate by direct DNA binding, we constructed GAL4-IE1 hybrids in which the GAL4 DBD (residues 1 to 147) was fused to IE1 (Fig. 1A). Placed under control of the *ie-1* promoter, the *gal4–ie-1* gene fusions were tested for the capacity to transactivate a viral promoter that contained tandem upstream GAL4 DNA binding sites, allowing direct interaction between IE1 and the promoter. GAL4-IE1 transactivation was monitored in transient expression assays in which SF21 cells were transfected with a reporter plasmid that contained the CAT gene under control of the basal promoter of the Ac*M*NPV *p35* gene with ($G_5 35K_{BAS}$-CAT) or without ($35K_{BAS}$-CAT) GAL4 DNA binding sites (Fig. 1B). The minimal *p35* basal promoter contains a TATA element and early RNA start site (+1) but lacks its viral upstream activating region (10, 39, 44).

GAL4-IE1(8-582), containing all but the first seven residues of IE1, transactivated the *p35* basal promoter in a GAL4-binding-site-dependent manner (Fig. 1C). This full-length IE1 fusion exhibited low-level reporter transactivation in the ab-

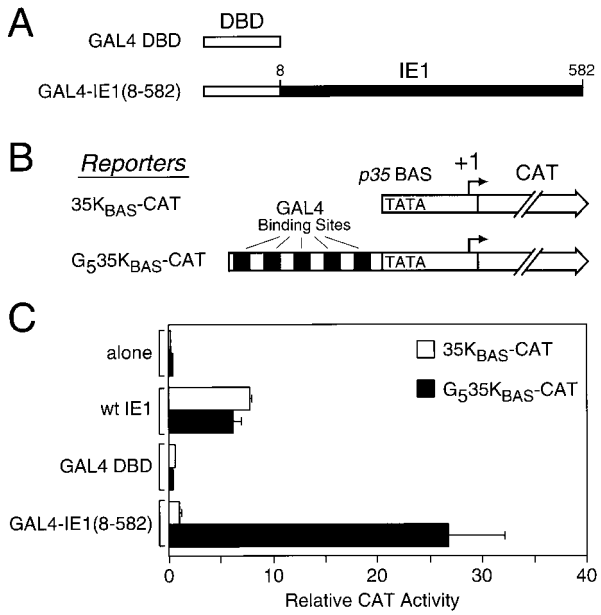

FIG. 1. GAL4-dependent IE1 transactivation. (A) Structure of GAL4-IE1(8-582). Sequences encoding the GAL4 DBD from amino acids 1 to 147 (open bar) were fused to IE1 sequences encoding residues 8 to 582 (solid bar) and placed under control of the Ac*M*NPV *ie-1* promoter. (B) Reporter plasmids. 35K$_{BAS}$-CAT contains the *p35* basal (BAS) promoter (TATA box and RNA start site, +1) linked to the CAT gene (open arrow). G$_5$35K$_{BAS}$-CAT is identical to 35K$_{BAS}$-CAT except for the presence of five GAL4 binding sites (solid boxes) upstream from the TATA element. (C) Transactivation by GAL4-IE1(8-582). SF21 cells (2×10^6/plate) were transfected with 10 μg of the indicated reporter plasmid alone or with 1 μg of wild-type (wt) IE1, GAL4 DBD, or GAL4-IE1(8-582) plasmid. Cell lysates were prepared 48 h later and assayed for CAT activity. The values are averages ± standard deviations of duplicate transfections and are reported as relative CAT activity normalized to that from 35K$_{BAS}$-CAT with GAL4-IE1(8-582).

sence of GAL4 binding sites (35K$_{BAS}$-CAT) but stimulated reporter expression 27-fold when GAL4 binding sites were present (G$_5$35K$_{BAS}$-CAT). In contrast, the presence of GAL4 DNA binding sites had no effect on the capacity of wild-type IE1 to transactivate the *p35* basal promoter, since levels of G$_5$35K$_{BAS}$-CAT and 35K$_{BAS}$-CAT expression were similar (Fig. 1C). The reduced transactivation of the *p35* basal promoter lacking GAL4 sites by GAL4-IE1(8-582) compared to wild-type IE1 was likely due to differences in folding or stability of the larger fusion protein. The GAL4 DBD alone failed to stimulate either reporter, which was inactive in the absence of IE1. Collectively, these data demonstrated that GAL4-IE1 transactivation depended on GAL4-binding-site interaction and suggested that IE1 can transactivate by DNA binding in a sequence-specific manner.

Identification of IE1 domains sufficient for GAL4-IE1 transactivation. To map IE1 residues responsible for GAL4-targeted transactivation, various segments of IE1 were fused to the GAL4 DBD (Fig. 2A) and tested for transactivation of the GAL4-binding site-containing CAT reporter G$_5$35K$_{BAS}$-CAT (Fig. 2B). All GAL4-IE1 fusions that included residues between 8 and 118 stimulated reporter expression. In particular, GAL4-IE1(8-118) increased expression 500-fold over that of the GAL4 DBD alone, a level five times higher than that of full-length GAL4-IE1(8-582). Nonoverlapping fusions GAL4-IE1(8-51) and GAL4-IE1(53-217) also exhibited stimulatory activity, suggesting that the transactivation domain of IE1 is either multipartite or tolerant to partial deletion. In contrast, GAL4-IE1 fusions that contained IE1 residues 120 to 217, 217 to 414, and 217 to 582 exhibited no stimulatory activity. The possibility that these fusions containing residues 120 to 582 were unstable in transfected cells was not ruled out. However, the presence of these residues did not destabilize the full-length GAL4-IE1(8-582) fusion. Taken together, these data indicated that N-terminal IE1 residues are sufficient for GAL4-targeted transactivation. Since IE1 residues 1 to 8 are dispensable for transactivation (23), our data suggest that the IE1 transactivation domain(s) lies between residues 8 and 118.

DNA binding and oligomerization by IE1 deletions. Previous findings that dimeric IE1 interacts with the palindromic 28-mer suggested that both DNA binding and oligomerization contribute to *hr*-dependent transactivation by IE1. Thus, to further map IE1 domains involved in 28-mer binding and oligomerization, we first constructed a series of internal *ie-1* deletions (Fig. 3). The mutated forms of IE1 were synthesized by using coupled transcription-translation reactions and subsequently tested for binding to a 28-mer-containing *hr*5 DNA probe (Fig. 3) in EMSAs. This in vitro approach provided a means to stably synthesize IE1 mutations at comparable levels and circumvented potential in vivo instability (see below; also data not shown).

In EMSAs, IE1 deletion IE1$^{\Delta 9\text{-}52}$ bound as a homodimer to the 28-mer probe with an affinity similar to that of wild-type

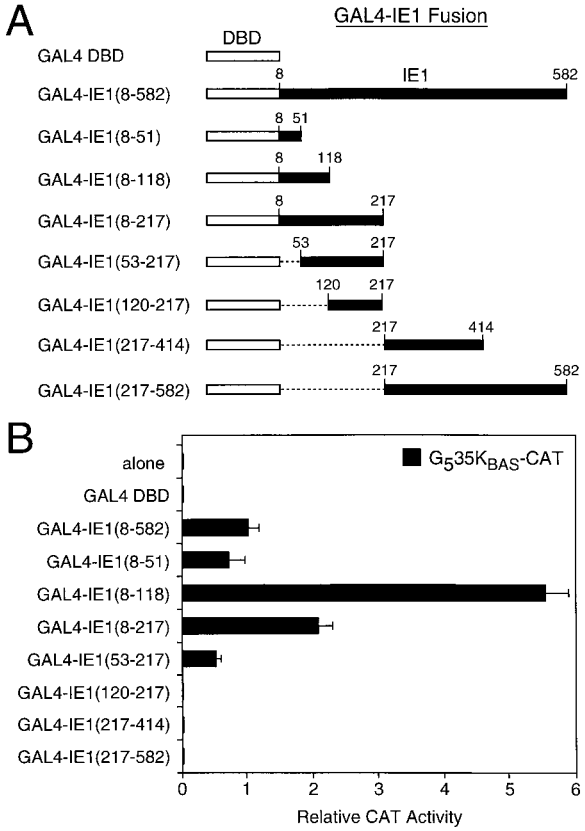

FIG. 2. Identification of IE1 transactivation domains. (A) Structure of GAL4-IE1 deletion proteins. The GAL4 DBD from amino acids 1 to 147 (open bar) was joined to segments of IE1 (solid bar) to generate GAL4-IE1 fusions that are designated by the indicated IE1 residues. (B) Transactivation by GAL4-IE1 fusion proteins. SF21 cells were transfected with reporter plasmid G$_5$35K$_{BAS}$-CAT alone or with the indicated GAL4-IE1 fusion plasmids and assayed for CAT activity as described in the legend to Fig. 1. The values are averages ± standard deviations of duplicate transfections and are reported as relative CAT activity normalized to that from GAL4-IE1(8-582).

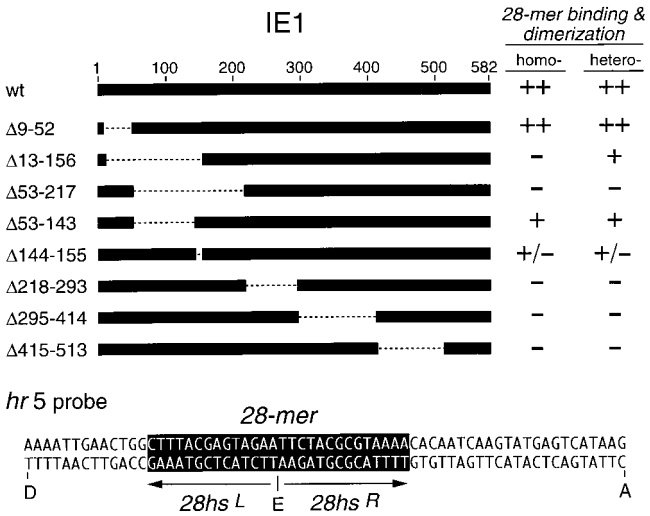

FIG. 3. Structure of IE1 deletions and 28-mer-containing *hr*5 DNA probe. Wild-type (wt) IE1 (solid bar) is shown above IE1 deletions designated by the amino acid residues removed (dashed line). As determined by EMSAs (Fig. 4), the ability (+) or inability (−) of each IE1 deletion to interact with the 28-mer DNA probe as a homodimer (homo-) or heterodimer (hetero-) with wild-type IE1 is indicated at the right. Nucleotides from *Dra*I to *Alu*I sites within the 131-bp DNA probe containing the leftmost 28-mer (boxed) of *hr*5 are shown. Left and right 28-mer half-sites ($28hs^L$ and $28hs^R$) are indicated by arrows. Restriction site abbreviations: A, *Alu*I; D, *Dra*I; E, *Eco*RI.

IE1 (Fig. 4A, lanes 2 and 3), as expected (45). The increased mobility of the complexes containing deleted IE1 is attributed to IE1's reduced size. In contrast to $IE1^{\Delta 9\text{-}52}$, all other IE1 deletions exhibited reduced or no 28-mer binding. Of these, $IE1^{\Delta 53\text{-}143}$ exhibited the highest level of homodimeric binding to the probe (lane 6). In addition, low-level binding of $IE1^{\Delta 144\text{-}155}$ was detected upon longer exposures (data not shown). Thus, the N-terminal 155 residues of IE1 are dispensable for minimal 28-mer interaction. Moreover, multiple regions within IE1 contribute directly or indirectly to complex formation.

To determine which IE1 deletions retained the capacity to oligomerize, in vitro-synthesized proteins were tested for heterodimerization with wild-type IE1 in 28-mer binding assays (Fig. 4B). As expected (45), $IE1^{\Delta 9\text{-}52}$ readily oligomerized with wild-type IE1 (lane 3), producing a heterodimeric DNA complex intermediate in mobility to $IE1^{\Delta 9\text{-}52}$ homodimers and wild-type IE1 homodimers (lane 2). Consistent with its ability to homodimerize, $IE1^{\Delta 53\text{-}143}$ also heterodimerized (lane 6) with wild-type IE1, forming an intermediate-size DNA complex. Due to size similarity, $IE1^{\Delta 144\text{-}155}$ heterodimers (lane 7) were indistinguishable from wild-type IE1 homodimers. Upon fusion of $IE1^{\Delta 144\text{-}155}$ to glutathione *S*-transferase, mixed subunits of glutathione *S*-transferase–$IE1^{\Delta 144\text{-}155}$ and IE1 were detected (data not shown). Although $IE1^{\Delta 13\text{-}156}$ failed to homodimerize, this deletion bound to the 28-mer as a heterodimer with wild-type IE1 (lane 4). However, all IE1 deletions that lacked residues C terminal to residue 156 failed to heterodimerize. Thus, N-terminal IE1 residues 9 to 155 are not required for IE1 oligomerization or DNA binding, but residues beyond 156 contribute directly or indirectly to both functions. The finding that deletion $IE1^{\Delta 13\text{-}156}$ bound DNA as a heterodimer but not as a homodimer also suggested that IE1 contains genetically separable DNA binding and oligomerization domains.

DNA binding and dimerization of insertion-mutated IE1. To disrupt local secondary structure and thereby more precisely map domains required for protein-protein or protein-DNA interactions, we next constructed a series of *ie-1* insertion mutations. *Bgl*II oligonucleotide linkers (8 to 12 bp) were placed throughout *ie-1* to generate IE1 mutations containing three to five amino acid insertions at unique locations (Fig. 5A). As determined by polyacrylamide gel electrophoresis of ^{35}S-labeled protein (Fig. 5B), the levels of in vitro-synthesized IE1 were similar for all insertions. Insertions $IE1^{I70}$, $IE1^{I118}$, $IE1^{I143}$, $IE1^{I414}$, $IE1^{I418}$, $IE1^{I513}$, and $IE1^{I579}$ independently bound to the 28-mer DNA probe with various affinities in EMSAs (Fig. 5C). $IE1^{143\Delta}$ (residues 144 to 145 replaced by Arg) also readily bound to the 28-mer probe. Longer exposures (not shown) were required to detect DNA binding by $IE1^{I311}$ and $IE1^{I462}$, suggesting reduced binding affinities. In contrast, $IE1^{I156}$, $IE1^{I245}$, $IE1^{I391}$, $IE1^{I425}$, and $IE1^{I553}$ failed to bind DNA. These data confirmed the multiplicity of IE1 domains contributing to DNA binding and the dispensability of the N-terminal 150 residues.

To determine which IE1 insertions retained the capacity to bind the 28-mer by heterodimerizing with a functional IE1, each was synthesized with the smaller functional $IE1^{\Delta 9\text{-}52}$ and subjected to EMSA (Fig. 5D). All IE1 insertions that independently bound DNA also formed heterodimers with $IE1^{\Delta 9\text{-}52}$. The level of heterodimerization (Fig. 5D) paralleled that of homodimerization (Fig. 5C). Although $IE1^{I156}$, $IE1^{I311}$, and $IE1^{I462}$ were impaired for 28-mer binding by themselves, each

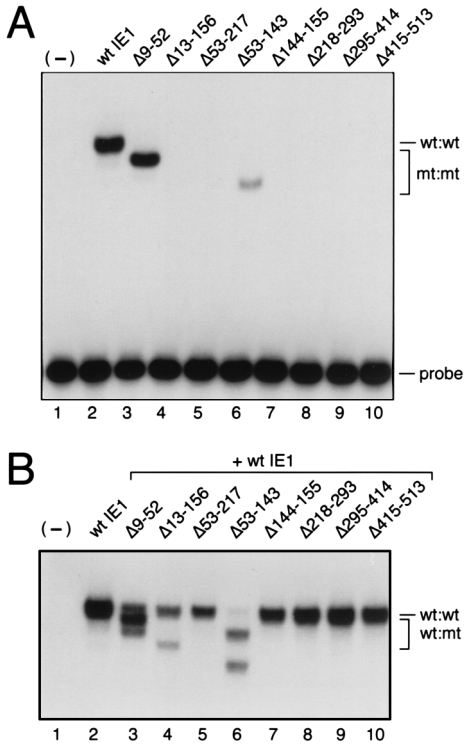

FIG. 4. EMSAs of IE1 deletions. (A) Homodimerization. ^{32}P-labeled 28-mer DNA probe was incubated with in vitro-synthesized wild-type (wt) IE1 (lane 2) or the indicated IE1 deletions (lanes 3 to 10) and subjected to EMSA by using nondenaturing polyacrylamide gel electrophoresis and autoradiography. DNA probe in the absence (−) of IE1 is shown (lane 1). (B) Heterodimerization with wild-type IE1. The indicated IE1 deletions were cosynthesized with wild-type IE1 and subjected to EMSA as described for panel A. The positions of IE1 heterodimers (wt:mt [wild type-mutant]) and wild-type IE1 homodimers (wt:wt) (lane 2) are indicated at the right. Unbound DNA probe is not shown.

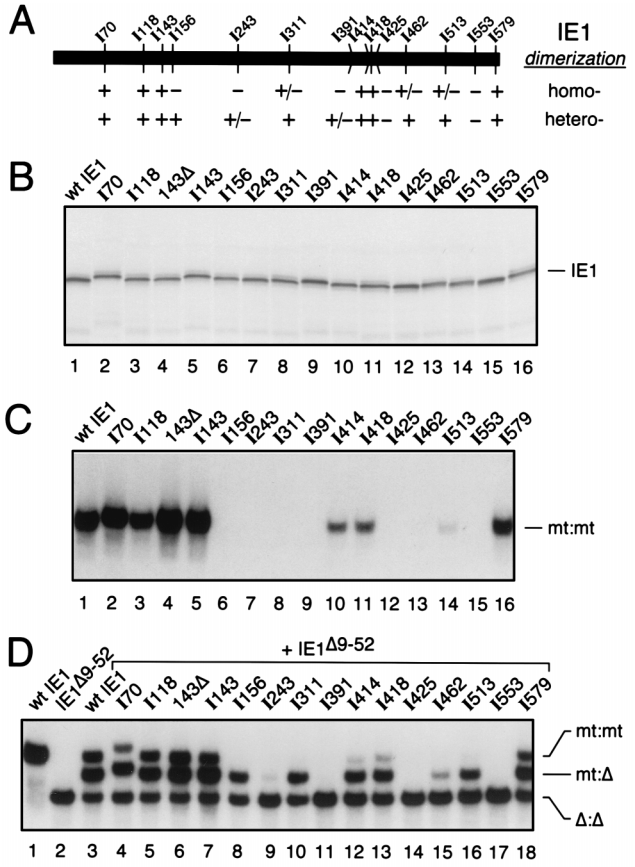

FIG. 5. EMSAs of insertion-mutated IE1. (A) Insertion mutations. IE1 mutations are designated by the position of the amino acid residue preceding the insertion. The ability (+) or inability (−) of mutated IE1 to interact with the 28-mer probe in EMSAs as a homodimer (C) or heterodimer with IE1$^{\Delta 9\text{-}52}$ (D) is summarized. (B) Quantitation of in vitro-synthesized IE1. ^{35}S-labeled wild-type (wt) IE1 and indicated IE1 insertion mutations were synthesized and subjected to sodium dodecyl sulfate (SDS)-polyacrylamide gel electrophoresis and fluorography. (C) Homodimerization. Wild-type (wt) IE1 and the indicated IE1 insertion mutants (mt) were independently synthesized and subjected to EMSA as described in the legend to Fig. 4. (D) Heterodimerization with IE1$^{\Delta 9\text{-}52}$. Wild-type IE1 and indicated IE1 insertions were cosynthesized with IE1$^{\Delta 9\text{-}52}$ and subjected to EMSA as described in the legend to Fig. 4. Wild-type (wt) IE1 (lane 1) and IE1$^{\Delta 9\text{-}52}$ (lane 2) alone were included. The positions of mutated homodimers (mt:mt), IE1$^{\Delta 9\text{-}52}$ homodimers (Δ:Δ), and mutant:IE1$^{\Delta 9\text{-}52}$ heterodimers (mt:Δ) are indicated at the right.

readily formed heterodimers with IE1$^{\Delta 9\text{-}52}$. Thus, these mutated IE1s contained a functional dimerization domain(s) and upon interaction with IE1$^{\Delta 9\text{-}52}$ did not interfere with its DNA binding. Both IE1^{I243} (lane 9) and IE1^{I391} (lane 11) heterodimerized only weakly; increased IE1$^{\Delta 9\text{-}52}$ was required to detect IE1^{I391} oligomers (data not shown). Lastly, IE1^{I425} and IE1^{I553} were the only insertions that failed to bind DNA either as homo- or heterodimers.

Dominant inhibition of IE1 DNA binding by IE1 insertions. Although the regions encompassing residues 425 and 553 are highly conserved among different baculovirus IE1 proteins, their sequence dissimilarity and relative separation suggested that these domains have different functions. To distinguish functions affected by the insertions, we compared the abilities of wild-type IE1, IE1^{I425}, and IE1^{I553} to interfere with 28-mer binding by functional IE1$^{\Delta 9\text{-}52}$. To this end, each IE1 was synthesized in increasing molar ratios of 1:1, 10:1, and 25:1 relative to IE1$^{\Delta 9\text{-}52}$ and tested for 28-mer binding by EMSAs. In the presence of excess DNA probe, a mutated IE1 with disrupted DNA binding activity, but unaffected oligomerization was predicted to competitively inhibit 28-mer binding by functional IE1. In contrast, disruption of oligomerization would cause reduced competition for DNA binding. As wild-type IE1 levels increased (Fig. 6, lanes 1 to 4), IE1$^{\Delta 9\text{-}52}$ homodimers disappeared and the level of wild-type IE1-IE1$^{\Delta 9\text{-}52}$ heterodimers increased and then stabilized. This pattern is consistent with competition between wild-type and IE1$^{\Delta 9\text{-}52}$ monomers for dimerization and DNA binding. With increasing levels of IE1^{I425} (Fig. 6, lanes 5 to 7), IE1$^{\Delta 9\text{-}52}$ homodimers were also depleted but without detection of DNA binding by heterodimers. This pattern suggested that IE1^{I425} associated with IE1$^{\Delta 9\text{-}52}$ but the resulting heterodimers were defective for 28-mer binding. In contrast, IE1$^{\Delta 9\text{-}52}$ homodimers were detected even in the presence of a 25-fold excess of IE1^{I553} (Fig. 6, lanes 8 to 10). Thus, IE1^{I553} failed to compete for IE1$^{\Delta 9\text{-}52}$ subunits as efficiently as wild-type IE1 or IE1^{I425}. These data suggested that the insertion at residue 425 disrupted DNA binding but not oligomerization, whereas the insertion at residue 553 abrogated IE1 oligomerization.

Requirement of a C-terminal hydrophobic 4-3 repeat for DNA binding. The failure of IE1^{I553} to either bind DNA or block binding by wild-type IE1 suggested that the region encompassing residue 553 is critical for dimerization. Inspection of potential secondary structure within this region reveals a positively charged domain (residues 521 to 544, pI of 11.74) that precedes two putative amphipathic α-helices (residues 543 to 572) consisting of 4-3 repeats of hydrophobic residues (Fig. 7A). This stretch within IE1 of Ac*M*NPV and *Orgyia pseudotsugata* multicapsid nuclear polyhedrosis virus (Op*M*NPV) matches a consensus basic–helix-loop-helix (b-HLH) motif required for oligomerization of other transcriptional activators (Fig. 7B). Insertion I553 interrupted the first helix, whereas deletion of the second helix caused loss of *hr*5 binding by IE1 (23). Thus, to better define the role of the b-HLH-like domain, we substituted hydrophobic residues within the 4-3 repeat with acidic residues (Asp or Glu) and replaced basic residues within the positively charged region with Ala (Fig. 7A). After verifying that the levels of in vitro-synthesized IE1 were similar for all substitutions (data not shown), each was assayed for 28-mer binding.

Substitution of hydrophobic residue pairs 543/547, 550/554, 561/564, and 565/568 within the IE1 4-3 repeats abolished 28-mer binding by each protein (IE1$^{L543D/L547E}$, IE1$^{L550D/I554E}$, IE1$^{L561D/A564E}$, and IE1$^{I565D/A568E}$) (Fig. 8A, lanes 3 to 6). Likewise, the 4-3 substitutions greatly reduced or eliminated

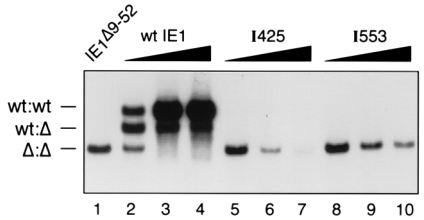

FIG. 6. Interference of IE1$^{\Delta 9\text{-}52}$ binding to the 28-mer. IE1$^{\Delta 9\text{-}52}$ was cosynthesized with increasing levels of wild-type (wt) IE1, IE1^{I425}, or IE1^{I553}, using molar ratios of 1:1 (lanes 2, 5, and 8), 1:10 (lanes 3, 6, and 9), and 1:25 (lanes 4, 7, and 10), and subjected to EMSA as described in the legend to Fig. 4. Constant DNA template concentrations were maintained by supplementing the in vitro synthesis reactions with a plasmid encoding luciferase under control of the SP6 promoter. The positions of wild-type IE1 homodimers (wt:wt), wild-type IE1:IE1$^{\Delta 9\text{-}52}$ heterodimers (wt:Δ), and IE1$^{\Delta 9\text{-}52}$ homodimers (Δ:Δ) are indicated at the left. Unbound DNA probe is not shown.

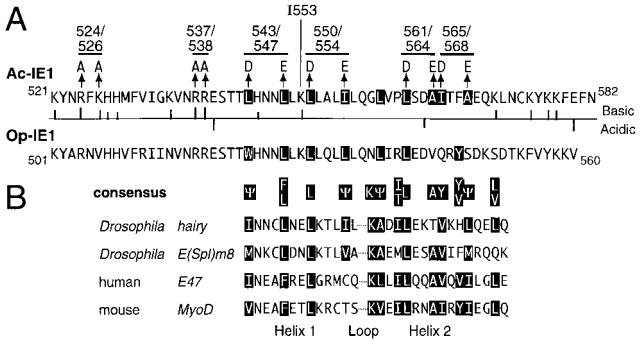

FIG. 7. (A) Amino acid substitutions within the putative dimerization domain of IE1. Pairs of residue substitutions designated by their positions are indicated above Ac*M*NPV IE1 (Ac-IE1) residues 521 to 582. Basic and acidic residues are indicated by vertical marks. Corresponding residues of Op*M*NPV IE1 (Op-IE1) are shown. (B) b-HLH domains. IE1 residues and those of four known b-HLH proteins are aligned with respect to the consensus sequence derived by Murre et al. (34); residues that match the consensus are highlighted. The predicted loop domains (dashed lines) vary in size. Nucleotide sequences: Ac*M*NPV IE1 (5, 18); *Drosophila hairy* (47); *Drosophila Enhancer of split [E(S-spl)m8]* (20); human *E47* (56); mouse *MyoD* (9). Ψ, hydrophobic residue.

the capacity of each mutated IE1 to bind DNA as a heterodimer with $IE1^{\Delta 9\text{-}52}$ (Fig. 8B, lanes 6 to 9); only $IE1^{I565D/A568E}$ and $IE1^{L550D/I554E}$ exhibited weak heterodimerization with $IE1^{\Delta 9\text{-}52}$. Thus, like insertion I553, substitution of hydrophobic residues within each predicted helix abolished DNA binding as both homo- and heterodimers. Substitution of adjacent Arg residues 537 and 538 on the N-terminal side of the 4-3 repeat also prevented DNA binding by $IE1^{R537A/R538A}$, either alone (Fig. 8A, lane 2) or with $IE1^{\Delta 9\text{-}52}$ (Fig. 8B, lane 5). In contrast, neither Arg^{524} or Lys^{526} was required for DNA binding, since $IE1^{R524A/K526A}$ bound DNA (Fig. 8A, lane 1) with an affinity comparable to that of wild-type IE1 (lane 7) and heterodimerized with $IE1^{\Delta 9\text{-}52}$ (Fig. 8B, lane 4). Thus, whereas Arg^{537} and Arg^{538} immediately adjacent to the 4-3 helices are required for DNA binding, basic residues N terminal to these helices are not.

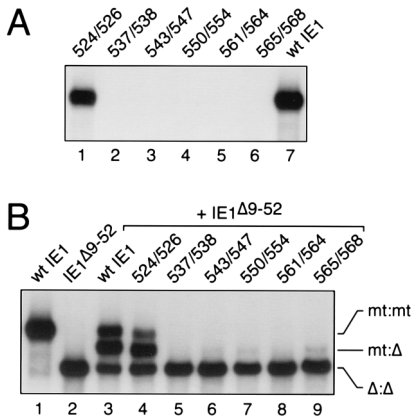

FIG. 8. DNA binding by b-HLH substitutions within IE1. (A) Homodimerization. The indicated IE1 amino acid substitutions were in vitro synthesized and subjected to EMSA as described in the legend to Fig. 4. (B) Heterodimerization with $IE1^{\Delta 9\text{-}52}$. Wild-type (wt) IE1 and the indicated IE1 substitutions were cosynthesized with $IE1^{\Delta 9\text{-}52}$ and subjected to EMSA. Wild-type IE1 (lane 1) and $IE1^{\Delta 9\text{-}52}$ alone (lane 2) were included. The positions of mutant homodimers (mt:mt), $IE1^{\Delta 9\text{-}52}$ homodimers (Δ:Δ), and mutant:$IE1^{\Delta 9\text{-}52}$ heterodimers (mt:Δ) are indicated at the right. Unbound DNA probe is not shown.

FIG. 9. IE1 functional domains. The 582-residue IE1 protein contains regions involved in transcriptional transactivation (residues 8 to 118), oligomerization (residues 543 to 568), and direct DNA binding which remain to be identified. Residues 432 and 512 that confer temperature sensitivity to *hr* binding by IE1 of Ac*M*NPV mutant *ts*B821 are also shown.

DISCUSSION

IE1 transactivation through DNA binding. The current model that IE1-mediated transactivation of the Ac*M*NPV *hr* enhancers requires DNA binding by IE1 is based on the finding that disruption of the minimal enhancer unit (28-mer) reduces IE1 binding and eliminates transcriptional enhancement (26, 45). However, it remained to be established that IE1 binding at or near a basal promoter induces transcriptional stimulation. By using constructed GAL4-IE1 fusions, we have shown here that IE1 interaction with a minimal TATA-containing promoter through binding to GAL4 DNA sites stimulated transcription. GAL4-IE1 transactivation was GAL4-binding-site dependent and conferred a 14- to 140-fold increase in expression, depending on the IE1 residues included (Fig. 1 and 2). Interaction of GAL4-IE1 fusions with the GAL4-binding-site-containing DNA was confirmed by EMSA (40). Thus, directed IE1 binding to a viral promoter was sufficient to activate transcription and further implies the involvement of DNA binding in IE1-mediated transactivation of 28-mer-linked viral promoters.

A common mechanism among transcriptional activators involves sequence-specific DNA binding that brings the activator into proximity with the promoter for assembly or stabilization of the transcription machinery (reviewed in references 2, 38, 46, 55, and 58). Transcriptional stimulation by virus-encoded activators is mediated by interaction with general host factors, including TATA binding protein and TFIIB (4, 12, 30, 33, 41, 49, 51). By analogy, it is likely that upon recruitment to a promoter, IE1 interacts with components of the basal transcription complex. Nonetheless, *hr* binding alone is not sufficient for IE1-mediated transactivation since 28-mer half-sites interact with IE1 but lack enhancer activity (14, 44, 45). Rather, IE1 binding to half-sites can inhibit transcription from Ac*M*NPV promoters (27). Thus, molecular events other than DNA binding are required for IE1 transactivation and remain to be defined.

IE1 domain(s) sufficient for transactivation. GAL4 DBD fusions with various transcriptional activators have been used to identify residues involved in transactivation (11, 19, 29, 37, 48, 50). By testing GAL4 fusions containing different segments of IE1 (Fig. 2), we have mapped the IE1 transactivation domain(s) to residues 8 through 118 (Fig. 9). Resembling the acidic transactivation domains of other transcriptional activators (reviewed in reference 53), the N-terminal stretch of IE1 from residues 8 to 118 is highly acidic, containing 18% Asp and Glu residues (−15 net charge) (18). GAL4-IE1 fusions containing nonoverlapping residues 8 to 51 and 53 to 217 also exhibited GAL4-dependent transactivation, although at levels lower than that conferred by residues 8 to 118. Thus, the entire acidic stretch was not required for transcriptional stimulation and suggested the presence of multiple transactivating domains. A similar division of acidic residues exists within the

activation domain of herpes simplex virus virion protein VP16, in which aromatic and hydrophobic residues are also critical (42, 48). IE1 residues 120 to 582 were not required for GAL4 transactivation, nor did these residues exhibit independent transactivation of the basal promoter (Fig. 2). Thus, our data suggest that IE1 residues sufficient for transactivation are confined to the N terminus (Fig. 9). These findings are consistent with a previous study that used progressive truncations to show that the IE1 N terminus is required for transactivation of *hr*-linked viral promoters (23).

IE1 residues required for 28-mer interaction. Consistent with the dispensability of the IE1 N terminus for DNA binding (23), mutated forms of IE1 with deletions or insertions between residues 9 to 155 retained the capacity to bind a 28-mer-containing DNA probe in EMSAs (Fig. 4 and 5). Whereas removal of IE1 residues 9 to 52 had little effect, removal of residues 53 to 143 or 144 to 155 reduced 28-mer binding (Fig. 4A). Residues 53 to 155 may therefore contribute to DNA binding but are not essential. In contrast, all internal deletions that removed IE1 sequences C-terminal to residue 155 eliminated 28-mer binding (Fig. 3 and 4). Thus, multiple IE1 domains are involved in DNA binding or participate indirectly by contributing to protein structure. This conclusion was supported by the finding that multiple insertion mutations outside the N-terminal transactivation domain impaired homodimeric binding of the 28-mer (Fig. 5A and C).

Among the IE1 insertions that failed to bind DNA as homodimers, two distinct classes were identified. The first class (including IE1^{I156}, IE1^{I243}, IE1^{I391}, and IE1^{I462}) bound DNA but only as heterodimers with IE1$^{\Delta 9\text{-}52}$. On the basis of their capacity to bind DNA by association with functional IE1, these insertions contained a functional oligomerization domain. Thus, each mutation either disrupted a DBD or altered IE1 structure that abolished DNA binding but not oligomerization. It is noteworthy that each of the regions flanking insertions at residues 156, 243, 391, and 462 is conserved among nuclear polyhedrosis virus *ie-1* genes. Of particular interest is the region flanking residue 156, which because of its high content of basic residues (6 of 10 and 9 of 17 Lys/Arg residues for Ac*M*NPV and Op*M*NPV IE1s, respectively) may be directly involved in contacting DNA. Consistent with a direct role in DNA binding, partial deletion of these basic residues (IE1$^{\Delta 13\text{-}156}$ and IE1$^{\Delta 144\text{-}155}$) or insertional disruption (IE1^{I156}) caused loss of homodimeric DNA binding but not oligomerization (Fig. 4 and 5).

The second class of IE1 insertion mutations (IE1^{I425} and IE1^{I553}) caused loss of homo- and heterodimeric binding to DNA (Fig. 5). In a manner analogous to wild-type IE1, excess IE1^{I425} interfered with 28-mer binding by functional IE1$^{\Delta 9\text{-}52}$, suggesting an interaction between both proteins (Fig. 6). However, the absence of detectable mixed-subunit complexes (IE1^{I425}-IE1$^{\Delta 9\text{-}52}$) indicated that this protein interaction impeded DNA binding by heterodimeric IE1$^{\Delta 9\text{-}52}$. Consistent with a critical role in IE1 function, the region flanked by residue 425 is highly conserved (15 of 16 residues are identical between Ac*M*NPV and Op*M*NPV IE1) (52) and is the location of the substitution A^{432}V (Fig. 9) that confers temperature sensitivity to *hr* binding by IE1 of Ac*M*NPV mutant *ts*B821 (7, 43). In contrast to IE1^{I425}, insertion IE1^{I553} failed to associate with functional IE1 and block 28-mer binding (Fig. 6). This property suggested that IE1^{I553}'s loss of DNA binding activity was due to disruption of oligomerization.

IE1 oligomerization. The observed restoration of DNA binding activity of IE1 insertions defective for homodimeric binding to the 28-mer (IE1^{I156}, IE1^{I243}, IE1^{I391}, and IE1^{I462}) by association with functional IE1 argues that oligomerization is critical to DNA binding. Supporting this conclusion was the finding that insertion I553 as well as substitutions of hydrophobic residues within the 4-3 repeat extending from IE1 residues 543 to 568 severely impaired homo- and heterodimeric binding of IE1 to DNA (Fig. 8). By analogy to the b-HLH motifs of other transcriptional activators (34), the hydrophobic face of the predicted IE1 α-helices (Fig. 7) is expected to be involved in protein-protein interaction. Thus, the loss of homo- and heterodimeric DNA binding by mutations that disrupted the putative IE1 helices is attributed to elimination of oligomerization. It remains to be shown whether the C-terminal b-HLH-like motif is required for IE1 dimerization in the absence of DNA binding. Kovacs et al. showed that deletion of IE1 residues 557 to 582 abolished *hr*5 binding by IE1 from transfected cell extracts (23). Our study thus attributes the loss of *hr*5 binding to defective oligomerization.

By analogy to b-HLH proteins, it was expected that the basic residues preceding the putative HLH motif of IE1 would contribute to IE1 DNA binding but not dimerization. Although substitution R^{537}A/R^{538}A failed to bind the 28-mer as a homodimer or as a heterodimer with IE1$^{\Delta 9\text{-}52}$, substitution R^{524}A/K^{526}A exhibited wild-type DNA binding (Fig. 8). Thus, the IE1 residues that participate in direct DNA binding may be located elsewhere, possibly within the basic region flanking residue 156. Further studies are required to identify the IE1 residues involved in DNA binding (Fig. 9) and to define the molecular mechanism wherein DNA binding is an obligatory step in IE1-mediated transactivation of the Ac*M*NPV *hr* enhancers.

ACKNOWLEDGMENTS

S.M.R. and S.S.P. contributed equally to this work.

This work was supported in part by Public Health Service grant AI25557 from the National Institute of Allergy and Infectious Diseases and NIH Predoctoral Traineeship GM07215 (to S.S.P.).

REFERENCES

1. **Ayres, M. D., S. C. Howard, J. Kuzio, F. M. Lopez, and R. D. Possee.** 1994. The complete DNA sequence of *Autographa californica* nuclear polyhedrosis virus. Virology **202:**586–605.
2. **Burley, S. K., and R. G. Roeder.** 1996. Biochemistry and structural biology of transcription factor IID (TFIID). Annu. Rev. Biochem. **65:**769–799.
3. **Carson, D. D., M. D. Summers, and L. A. Guarino.** 1991. Transient expression of the *Autographa californica* nuclear polyhedrosis virus immediate-early gene, IE-N, is regulated by three viral elements. J. Virol. **65:**945–951.
4. **Caswell, R., C. Hagemeier, C. J. Chiou, G. Hayward, T. Kouzarides, and J. Sinclair.** 1993. The human cytomegalovirus 86K immediate early (IE) 2 protein requires the basic region of the TATA-box binding protein (TBP) for binding, and interacts with TBP and transcription factor TFIIB via regions of IE2 required for transcriptional regulation. J. Gen. Virol. **74:**2691–2698.
5. **Chisholm, G. E., and D. J. Henner.** 1988. Multiple early transcripts and splicing of the *Autographa californica* nuclear polyhedrosis virus IE-1 gene. J. Virol. **62:**3193–3200.
6. **Choi, J., and L. A. Guarino.** 1995. The baculovirus transactivator IE1 binds to viral enhancer elements in the absence of insect cell factor. J. Virol. **69:**4548–4551.
7. **Choi, J., and L. A. Guarino.** 1995. A temperature-sensitive IE1 protein of *Autographa californica* nuclear polyhedrosis virus has altered transactivation and DNA binding activities. Virology **209:**90–98.
8. **Cochran, M. A., and P. Faulkner.** 1983. Location of homologous DNA sequences interspersed at five regions in the baculovirus AcMNPV genome. J. Virol. **45:**961–970.
9. **Davis, R. L., H. Weintraub, and A. B. Lassar.** 1987. Expression of a single transfected cDNA converts fibroblasts to myoblasts. Cell **51:**987–1000.
10. **Dickson, J. A., and P. D. Friesen.** 1991. Identification of upstream promoter elements mediating early transcription from the 35,000-molecular-weight protein gene of *Autographa californica* nuclear polyhedrosis virus. J. Virol. **65:**4006–4016.
11. **Flemington, E. K., A. M. Borras, J. P. Lytle, and S. H. Speck.** 1992. Characterization of the Epstein-Barr virus BZLF1 protein transactivation domain. J. Virol. **66:**922–929.
12. **Gruda, M. C., J. M. Zabolotny, J. H. Xiao, I. Davidson, and J. C. Alwine.** 1993. Transcriptional activation by simian virus 40 large T antigen: interac-

tions with multiple components of the transcription complex. Mol. Cell. Biol. **13:**961–969.
13. **Guarino, L. A., and W. Dong.** 1991. Expression of an enhancer-binding protein in insect cells transfected with the *Autographa californica* nuclear polyhedrosis virus IE1 gene. J. Virol. **65:**3676–3680.
14. **Guarino, L. A., and W. Dong.** 1994. Functional dissection of the *Autographa californica* nuclear polyhedrosis virus enhancer element hr5. Virology **200:** 328–335.
15. **Guarino, L. A., M. A. Gonzalez, and M. D. Summers.** 1986. Complete sequence and enhancer function of the homologous DNA regions of *Autographa californica* nuclear polyhedrosis virus. J. Virol. **60:**224–229.
16. **Guarino, L. A., and M. D. Summers.** 1986. Functional mapping of a *trans*-activating gene required for expression of a baculovirus delayed-early gene. J. Virol. **57:**563–571.
17. **Guarino, L. A., and M. D. Summers.** 1986. Interspersed homologous DNA of *Autographa californica* nuclear polyhedrosis virus enhances delayed-early gene expression. J. Virol. **60:**215–223.
18. **Guarino, L. A., and M. D. Summers.** 1987. Nucleotide sequence and temporal expression of a baculovirus regulatory gene. J. Virol. **61:**2091–2099.
19. **Hardwick, J. M., L. Tse, N. Applegren, J. Nicholas, and M. A. Veliuona.** 1992. The Epstein-Barr virus R transactivator (Rta) contains a complex, potent activation domain with properties different from those of VP16. J. Virol. **66:**5500–5508.
20. **Klambt, C., E. Knust, K. Tietze, and J. A. Campos-Ortega.** 1989. Closely related transcripts encoded by the gene complex *Enhancer of split* of *Drosophila melanogaster*. EMBO J. **8:**203–210.
21. **Kool, M., C. H. Ahrens, R. W. Goldbach, G. F. Rohrmann, and J. M. Vlak.** 1994. Identification of genes involved in DNA replication of the *Autographa californica* baculovirus. Proc. Natl. Acad. Sci. USA **91:**11212–11216.
22. **Kool, M., J. T. Voeten, R. W. Goldbach, J. Tramper, and J. M. Vlak.** 1993. Identification of seven putative origins of *Autographa californica* multiple nucleocapsid nuclear polyhedrosis virus DNA replication. J. Gen. Virol. **74:**2661–2668.
23. **Kovacs, G. R., J. Choi, L. A. Guarino, and M. D. Summers.** 1992. Functional dissection of the *Autographa californica* nuclear polyhedrosis virus immediate-early 1 transcriptional regulatory protein. J. Virol. **66:**7429–7437.
24. **Kovacs, G. R., L. A. Guarino, and M. D. Summers.** 1991. Novel regulatory properties of the IE1 and IE0 transactivators encoded by the baculovirus *Autographa californica* multicapsid nuclear polyhedrosis virus. J. Virol. **65:** 5281–5288.
25. **Kunkel, T. A., J. D. Roberts, and R. A. Zakour.** 1987. Rapid and efficient site-specific mutagenesis without phenotypic selection. Methods Enzymol. **154:**367–382.
26. **Leisy, D. J., C. Rasmussen, H.-T. Kim, and G. F. Rohrmann.** 1995. The *Autographa californica* nuclear polyhedrosis virus homologous region 1a: identical sequences are essential for DNA replication activity and transcriptional enhancer function. Virology **208:**742–752.
27. **Leisy, D. J., C. Rasmussen, E. O. Owusu, and G. F. Rohrmann.** 1997. A mechanism for negative gene regulation in *Autographa californica* nuclear polyhedrosis virus. J. Virol. **71:**5088–5094.
28. **Leisy, D. J., and G. F. Rohrmann.** 1993. Characterization of the replication of plasmids containing hr sequences in baculovirus-infected *Spodoptera frugiperda* cells. Virology **196:**722–730.
29. **Lillie, J. W., and M. R. Green.** 1989. Transcription activation by the adenovirus E1a protein. Nature **338:**39–44.
30. **Lin, Y. S., I. Ha, E. Maldonado, D. Reinberg, and M. R. Green.** 1991. Binding of general transcription factor TFIIB to an acidic activating region. Nature **353:**569–571.
31. **Lu, A., and E. B. Carstens.** 1993. Immediate-early baculovirus genes transactivate the p143 gene promoter of *Autographa californica* nuclear polyhedrosis virus. Virology **195:**710–718.
32. **Lu, A., and L. K. Miller.** 1995. The roles of eighteen baculovirus late expression factor genes in transcription and DNA replication. J. Virol. **69:**975–982.
33. **Manet, E., C. Allera, H. Gruffat, I. Mikaelian, A. Rigolet, and A. Sergeant.** 1993. The acidic activation domain of the Epstein-Barr virus transcription factor R interacts in vitro with both TBP and TFIIB and is cell-specifically potentiated by a proline-rich region. Gene Expr. **3:**49–59.
34. **Murre, C., P. S. McCaw, and D. Baltimore.** 1989. A new DNA binding and dimerization motif in immunoglobulin enhancer binding, daughterless, MyoD, and myc proteins. Cell **56:**777–783.
35. **Nissen, M. S., and P. D. Friesen.** 1989. Molecular analysis of the transcriptional regulatory region of an early baculovirus gene. J. Virol. **63:**493–503.
36. **Pearson, M. N., R. M. Bjornson, C. Ahrens, and G. F. Rohrmann.** 1993. Identification and characterization of a putative origin of DNA replication in the genome of a baculovirus pathogenic for *Orgyia pseudotsugata*. Virology **197:**715–725.
37. **Pizzorno, M. C., M. A. Mullen, Y. N. Chang, and G. S. Hayward.** 1991. The functionally active IE2 immediate-early regulatory protein of human cytomegalovirus is an 80-kilodalton polypeptide that contains two distinct activator domains and a duplicated nuclear localization signal. J. Virol. **65:**3839–3852.
38. **Ptashne, M., and A. Gann.** 1997. Transcriptional activation by recruitment. Nature **386:**569–577.
39. **Pullen, S. S., and P. D. Friesen.** 1995. Early transcription of the IE-1 transregulator gene of *Autographa californica* nuclear polyhedrosis virus is regulated by DNA sequences within its 5′ noncoding leader region. J. Virol. **69:**156–165.
40. **Pullen, S. S., and P. D. Friesen.** Unpublished data.
41. **Qadri, I., H. F. Maguire, and A. Siddiqui.** 1995. Hepatitis B virus transactivator protein X interacts with the TATA-binding protein. Proc. Natl. Acad. Sci. USA **92:**1003–1007.
42. **Regier, J. L., F. Shen, and S. J. Triezenberg.** 1993. Pattern of aromatic and hydrophobic amino acids critical for one of two subdomains of the VP16 transcriptional activator. Proc. Natl. Acad. Sci. USA **90:**883–887.
43. **Ribeiro, B. M., K. Hutchinson, and L. K. Miller.** 1994. A mutant baculovirus with a temperature-sensitive IE-1 transregulatory protein. J. Virol. **68:**1075–1084.
44. **Rodems, S. M., and P. D. Friesen.** 1993. The *hr*5 transcriptional enhancer stimulates early expression from the *Autographa californica* nuclear polyhedrosis virus genome but is not required for virus replication. J. Virol. **67:** 5776–5785.
45. **Rodems, S. M., and P. D. Friesen.** 1995. Transcriptional enhancer activity of *hr*5 requires dual-palindrome half sites that mediate binding of a dimeric form of the baculovirus transregulator IE1. J. Virol. **69:**5368–5375.
46. **Roeder, R. G.** 1996. The role of general initiation factors in transcription by RNA polymerase II. Trends Biochem. Sci. **21:**327–335.
47. **Rushlow, C. A., A. Hogan, S. M. Pinchin, K. M. Howe, M. Lardelli, and D. Ish-Horowicz.** 1989. The *Drosophila hairy* protein acts in both segmentation and bristle patterning and shows homology to N-*myc*. EMBO J. **8:**3095–3103.
48. **Sadowski, I., J. Ma, S. Triezenberg, and M. Ptashne.** 1988. GAL4-VP16 is an unusually potent transcriptional activator. Nature **335:**563–564.
49. **Smith, C. A., P. Bates, R. Rivera-Gonzalez, B. Gu, and N. A. DeLuca.** 1993. ICP4, the major transcriptional regulatory protein of herpes simplex virus type 1, forms a tripartite complex with TATA-binding protein and TFIIB. J. Virol. **67:**4676–4687.
50. **Southgate, C. D., and M. R. Green.** 1991. The HIV-1 Tat protein activates transcription from an upstream DNA-binding site: implications for Tat function. Genes Dev. **5:**2496–2507.
51. **Steger, G., J. Ham, O. Lefebvre, and M. Yaniv.** 1995. The bovine papillomavirus 1 E2 protein contains two activation domains: one that interacts with TBP and another that functions after TBP binding. EMBO J. **14:**329–340.
52. **Theilmann, D. A., and S. Stewart.** 1991. Identification and characterization of the IE-1 gene of *Orgyia pseudotsugata* multicapsid nuclear polyhedrosis virus. Virology **180:**492–508.
53. **Triezenberg, S. J.** 1995. Structure and function of transcriptional activation domains. Curr. Opin. Genet. Dev. **5:**190–196.
54. **Vaughn, J. L., R. H. Goodwin, G. J. Tompkins, and P. McCawley.** 1977. The establishment of two cell lines from the insect *Spodoptera frugiperda* (Lepidoptera; Noctuidae). In Vitro **13:**213–217.
55. **Verrijzer, C. P., and R. Tjian.** 1996. TAFs mediate transcriptional activation and promoter selectivity. Trends Biochem. Sci. **21:**338–342.
56. **Voronova, A., and D. Baltimore.** 1990. Mutations that disrupt DNA binding and dimer formation in the E47 helix-loop-helix protein map to distinct domains. Proc. Natl. Acad. Sci. USA **87:**4722–4726.
57. **Wade Harper, J., G. R. Adami, N. Wei, K. Keyomarsi, and S. J. Elledge.** 1993. The p21 cdk-interacting protein Cip1 is a potent inhibitor of G1 cyclin-dependent kinases. Cell **75:**805–816.
58. **Zawel, L., and D. Reinberg.** 1995. Common themes in assembly and function of eukaryotic transcription complexes. Annu. Rev. Biochem. **64:**533–561.